



Synthesis and properties of catechol-fused tetrathiafulvalene derivatives and their hydrogen-bonded conductive charge-transfer salts

Hiromichi Kamo^{a,*}, Akira Ueda^{a,*}, Takayuki Isono^a, Kazuyuki Takahashi^b, Hatsumi Mori^{a,*}

^aThe Institute for Solid State Physics, The University of Tokyo, Kashiwa, Chiba 277-8581, Japan

^bDepartment of Chemistry, Graduate School of Science, Kobe University, Kobe, Hyogo 657-8501, Japan

ARTICLE INFO

Article history:

Received 10 May 2012

Revised 4 June 2012

Accepted 6 June 2012

Available online 13 June 2012

Keywords:

Tetrathiafulvalene

Catechol

Charge-transfer salt

Hydrogen bond

Electrical resistivity

ABSTRACT

Catechol-fused tetrathiafulvalene (TTF) derivatives have been designed and synthesized as a new type of π -electron donor molecules having two phenolic hydroxyl groups. Cyclic voltammetry measurements and quantum chemical calculations demonstrated the electronic effect of the direct fusion of the catechol unit to the TTF π -skeleton. In the charge-transfer (CT) salts with bromide or chloride anions, a one-dimensional hydrogen-bonded chain was formed by the intermolecular $\text{OH} \cdots \text{X}$ network between the catechol moieties and the halide anions. The slight dissimilarity of the hydrogen-bond distances for the two CT salts gave rise to the significant differences in their overall molecular arrangements and intermolecular interactions as well as the electrical resistivities.

© 2012 Elsevier Ltd. All rights reserved.

Tetrathiafulvalene (TTF), a well-known strong organic electron donor molecule with a planar π -conjugated skeleton, and its derivatives have been extensively studied as a promising component of functional solids and materials that show (super)conductivity, magnetism, dielectric and optical properties, etc.¹ Chemists have devoted a lot of efforts to functionalize TTF-based π -electronic molecules to explore unique structural and electronic features and physical properties attributable to combination effects of the parent TTF system with the introduced functional groups or substituents.^{1–4} For example, a number of TTF derivatives bearing hydrogen-bonding functionalities, such as alcohols,^{3a–c} (thio)amides,^{3d–g} nucleobases,^{3h–j} and heterocycles,^{3k–m} have been designed and synthesized so far. In their charge-transfer (CT) salts and complexes, such hydrogen-bonding functionalities made a significant contribution to control the electronic state, molecular arrangements, and solid-state physical properties.^{3,4}

Catechol is a well-known aromatic molecule that has two phenolic hydroxyl groups at the neighboring positions of a benzene ring. Because of this structural feature, this system can act not only as chelating ligands, such as semiquinone and catecholate, in the metal complexes,⁵ but also as an anion binder or receptor with an $\text{OH} \cdots \text{X}$ hydrogen bond.⁶ Therefore we have designed catechol-fused TTF derivatives **1** as new type of π -electron donor molecules having hydrogen bonding and metal binding abilities

(Fig. 1). By directly fusing the catechol unit to the TTF skeleton, we especially expect that the electronic state of the TTF π -skeleton and the overall bulk physical properties of the **1**-based molecular system can be significantly changed depending on the hydroxyl-group environment of the catechol moiety. In contrast to a lot of studies on the TTF derivatives having a hydroxyl group linked by a σ -bond,^{3a–c,4} those linked by a π -conjugated system have rarely been reported.⁷ Here we report the synthesis and properties of the first catechol-fused TTF derivatives **1** and their hydrogen-bonded charge transfer salts.

The synthesis of catechol-fused TTF derivatives **1a–e** and diselenadithiafulvalene (STF) derivative **1f** was achieved by the five-step synthetic protocol from 1,2-bis(benzyloxy)-4,5-dibromobenzene⁸ (Scheme 1). The Stille-type cross-coupling reaction of the dibromobenzene derivative with 3-[(tributylstannyl)thio]propanenitrile⁹ quantitatively gave the bis(2-cyanoethylthio) derivative **2**.

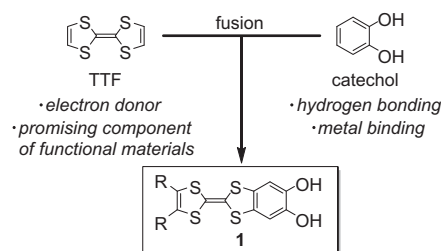
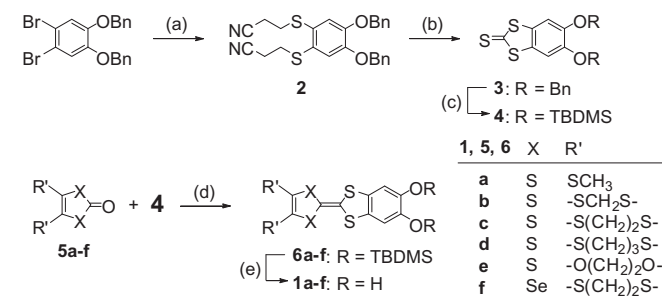


Figure 1. Molecular design of catechol-fused TTF derivatives **1**.

* Corresponding authors. Tel./fax: +81 4 7136 3410 (H.K., A.U.); tel./fax: +81 4 7136 3444 (H.M.)

E-mail addresses: a-ueda@issp.u-tokyo.ac.jp (A. Ueda), hmori@issp.u-tokyo.ac.jp (H. Mori).



Scheme 1. Synthesis of catechol-fused TTF derivatives **1a–f**. Reagents and conditions: (a) ^tBu₃SnS(CH₂)₂CN, Pd(PPh₃)₄, toluene, reflux, 95%; (b) (i) NaOMe, ZnCl₂, Bu₄NBr, MeOH, CH₂Cl₂, room temperature, (ii) 1,1'-thiocarbonyldiimidazole, AcOH, THF, −78 °C–room temperature, 60%; (c) (i) BF₃·Et₂O, ^tBuSH, CHCl₃, 60 °C, (ii) AcOH, MeOH, 60 °C, (iii) TBDMSCl, Et₃N, *N,N*-dimethyl-4-aminopyridine, CH₂Cl₂, room temperature, 53%; (d) P(OEt)₃, 100–110 °C, 14–56%; (e) Bu₄NF, AcOH, THF, room temperature, 36–79%.

The treatment of **2** with NaOMe and ZnCl₂ followed by the reaction with 1,1'-thiocarbonyldiimidazole under an acidic condition yielded the 1,3-benzodithiole-2-thione derivative **3**. The benzyl protecting groups of **3** were removed by BF₃·Et₂O and *n*BuSH¹⁰ and the subsequent reprotection by TBDMS groups afforded **4**.¹¹ Finally the target compounds **1a–f** were obtained¹² by the cross-coupling reaction between **4** and the corresponding ketone **5a–f** in P(OEt)₃ and the following deprotection of the TBDMS groups. These donors **1a–f** are stable in the solid state in air at −20 °C for a few months, whereas a solution of **1a–f** gradually decomposes under an aerobic condition. This synthetic scheme can be applicable to explore further various kinds of asymmetric TTF derivatives with a benzo-fused π -electronic structure by using an appropriate 1,2-dibromobenzene derivative as the starting material.

To evaluate electrochemical properties of this system, we measured cyclic voltammograms of **1a–f** in a CH₃CN solution. Similar to typical TTF derivatives, all the donor molecules **1a–f** exhibited two reversible oxidation waves. As listed in Table 1, the first and second oxidation potentials ($E^{1/2}$, $E^{2/2}$) of **1a–f** vary to some extent (+0.35 to +0.48 V and +0.62 to +0.76 V, respectively), indicating that the HOMO energy level changes depending on the substituents R' at the TTF skeleton. In contrast, differences between two oxidation potentials ΔE ($=E^{2/2}-E^{1/2}$) are similar to each other (0.24–0.28 V). This result means that the on-site Coulomb repulsion energy in **1a–f** is almost unchanged in spite of the difference in R'. Namely the on-site Coulomb repulsion energy of this system is mostly governed by the catechol-fused TTF π -conjugated structure itself. Furthermore, to investigate an electronic effect of the fused catechol moiety on the TTF system, we compared the $E^{1/2}$ and ΔE values of the ethylenedithio derivative **1c** with those of EDT-TTF^{13a} and Benzo-EDT-TTF^{13b} (Table 1, see also Fig. 2 for their chemical structures). The first oxidation potentials of **1c** (+0.40 V)

Table 1

The first and second oxidation potentials ($E^{1/2}$, $E^{2/2}$) and their differences ΔE ($=E^{2/2}-E^{1/2}$) for **1a–f** obtained by CV measurements (V vs SCE, glassy carbon working electrode with 0.1 M Bu₄NClO₄ in CH₃CN). The literature values for EDT-TTF^{13a} and Benzo-EDT-TTF^{13b} were also listed as reference

Compound	$E^{1/2}/V$	$E^{2/2}/V$	$\Delta E/V$
1a	+0.39	+0.64	0.25
1b	+0.41	+0.65	0.24
1c	+0.40	+0.65	0.25
1d	+0.43	+0.71	0.28
1e	+0.35	+0.62	0.27
1f	+0.48	+0.76	0.28
EDT-TTF ^{13a}	+0.42	+0.74	0.32
Benzo-EDT-TTF ^{13b}	+0.57	+0.87	0.30

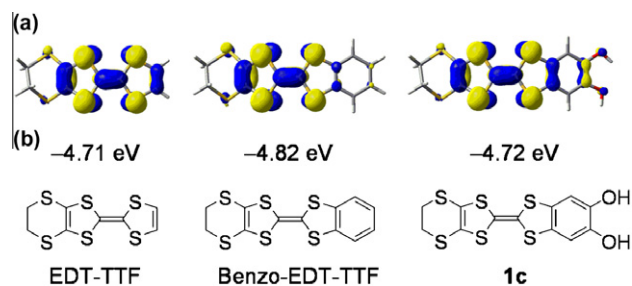


Figure 2. (a) HOMO pictures and (b) HOMO energy levels of EDT-TTF, Benzo-EDT-TTF, and **1c** calculated at the B3LYP/6-31G* level of theory.

and EDT-TTF (+0.42 V) are almost the same but significantly smaller than that of Benzo-EDT-TTF (+0.57 V). This result suggests that the HOMO energy level decreases by the benzo-annulation to the parent EDT-TTF skeleton, and then it increases by the introduction of two electron-donating hydroxyl groups into the benzene ring to form the catechol structure. Furthermore, we found that **1c** has a smaller ΔE value (0.25 V) than both EDT-TTF (0.32 V) and Benzo-EDT-TTF (0.30 V), indicating that the direct fusion of the catechol skeleton to the TTF system significantly contributes to an extension of the π -conjugated system, to lead to the decrease in ΔE , that is, the on-site Coulomb repulsion energy.

These electronic effects induced by the direct fusion of the catechol moiety were also illustrated by the density functional theory (DFT) calculations (Fig. 2).¹⁴ The HOMO coefficients of **1c** are widely distributed not only on the TTF skeleton but also on the catechol moiety including the two oxygen atoms (Fig. 2a). In contrast, there are much smaller coefficients on the benzene ring in Benzo-EDT-TTF. Thus the higher delocalization of HOMO in **1c** probably contributes to the decrease of the observed ΔE value. Furthermore the calculated HOMO energy levels of EDT-TTF (−4.71 eV), Benzo-EDT-TTF (−4.82 eV), and **1c** (−4.72 eV) (Fig. 2b) qualitatively reproduce the difference of their observed oxidation potentials (Table 1). All these experimental and calculated results demonstrate that a robust π -electronic communication exists between the TTF skeleton and the catechol moiety, as we expected.

In order to examine how the two phenolic hydroxyl groups of the introduced catechol moiety in **1** affect the intermolecular interaction and conductivity in the solid state, we attempted to prepare the charge transfer (CT) salts of **1a–f** with various inorganic anions by the electrochemical oxidation. As a result, two kinds of CT salts composed of the ethylenedithio derivative **1c** and chloride or bromide ion were successfully obtained as black plate crystals and black block crystals which are suitable for X-ray crystal analyses, respectively. Both salts crystallize in a space group of *P*-1 (triclinic) where two inversion-symmetric donor molecules **1c** and one halide ion exist in the unit cell.¹⁵ Thus the compositional formulae of these salts were determined as (**1c**)₂Cl and (**1c**)₂Br, respectively, indicating that the charge of the donor **1c** is +0.5 with a 1/4-filled band structure. This donor-anion ratio was also confirmed by the bond length analyses of the donor skeletons (see the Supplementary data). In each crystal, both two OH groups of the catechol unit participate in the OH...X (X = Cl, Br) intermolecular hydrogen bonds with the corresponding counter halide ions, respectively (Fig. 3a,b). The O...X distances are found to be O1-Cl = 3.23 Å, O2-Cl = 3.06 Å, O1-Br = 3.28 Å, and O2-Br = 3.31 Å, respectively, which all are shorter than the sum of their van der Waals radius (O-Cl: 3.27 Å, O-Br: 3.37 Å). Consequently the halide ions are surrounded by four hydroxyl groups in both crystals, to give an infinite one-dimensional (1D) chain structure along the *a*-axis. Although the hydrogen-bonding manners in (**1c**)₂Cl and (**1c**)₂Br are almost similar, their overall molecular arrangements are different (Fig. 3c,d). Namely, (**1c**)₂Cl and (**1c**)₂Br are categorized as β'' -type and β -type,

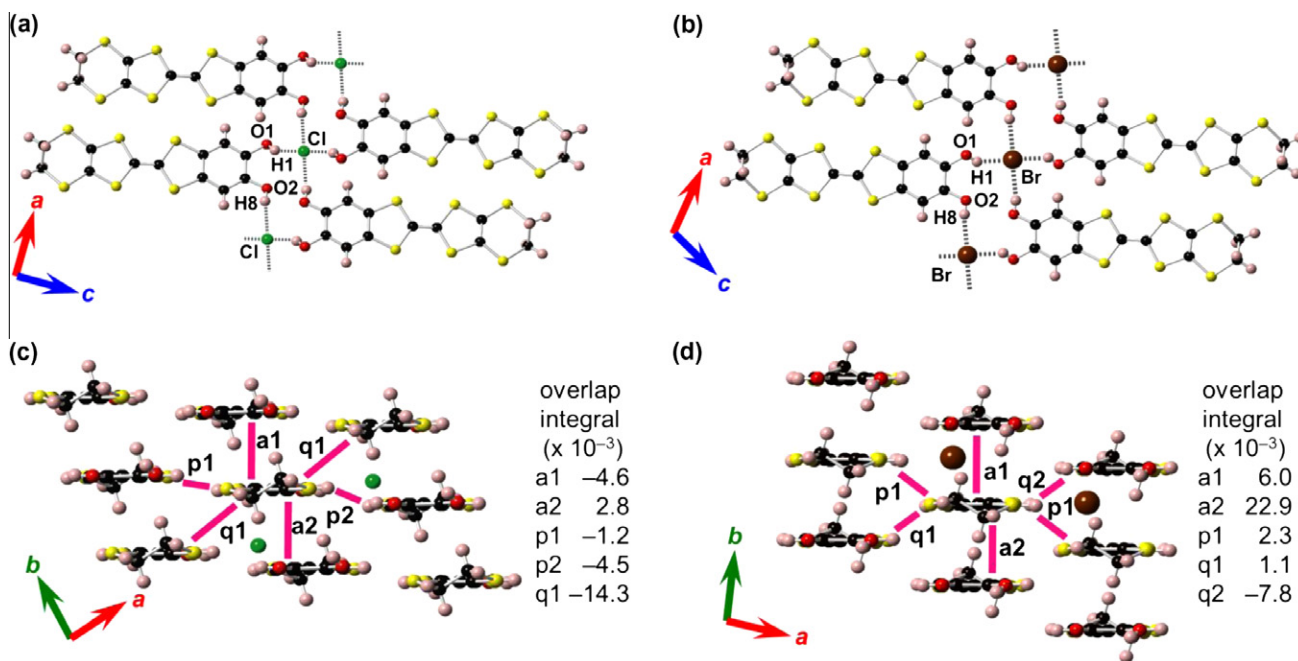


Figure 3. X-ray crystal structures of $(\mathbf{1c})_2\text{Cl}$ and $(\mathbf{1c})_2\text{Br}$. Hydrogen bonding motif along the b axis in (a) $(\mathbf{1c})_2\text{Cl}$ ($\text{O1-Cl} = 3.23 \text{ \AA}$ and $\text{O2-Cl} = 3.06 \text{ \AA}$) and in (b) $(\mathbf{1c})_2\text{Br}$ ($\text{O1-Br} = 3.28 \text{ \AA}$ and $\text{O2-Br} = 3.31 \text{ \AA}$). Molecular arrangement with the calculated overlap integrals of (c) $(\mathbf{1c})_2\text{Cl}$ and (d) $(\mathbf{1c})_2\text{Br}$. Black, yellow, red, pink, green, and brown spheres represent carbon, sulfur, oxygen, hydrogen, chlorine, and bromine atoms, respectively.

respectively.¹⁶ This difference is probably originating from the subtle difference in the hydrogen bond distances depending on the size of the halide ion. Then, to quantitatively estimate intermolecular interactions in the crystal, the overlap integrals between two donor skeletons were calculated by using its HOMO obtained by the extended Hückel method.^{17,18} As a result, it turns out that $(\mathbf{1c})_2\text{Cl}$ provides its largest value (-14.3×10^{-3}) in the q1 direction, in which the oxidized donors $\mathbf{1c}$ are connected by the hydrogen bonds through the Cl anion. In contrast, $(\mathbf{1c})_2\text{Br}$ shows a very small overlap integral between the hydrogen-bonded donors ($p1 = 2.3 \times 10^{-3}$) and the largest value is found in the a2 direction (22.9×10^{-3}). Thus $(\mathbf{1c})_2\text{Br}$ has a strong dimerization ($a2/a1 = 3.8$) in the b -direction in contrast to no dimerization ($q1 = -14.3 \times 10^{-3}$) for $(\mathbf{1c})_2\text{Cl}$.

These dissimilar intermolecular interactions also gave a significantly different conducting behavior of two salts $(\mathbf{1c})_2\text{Cl}$ and $(\mathbf{1c})_2\text{Br}$. The electrical resistivity measurements of the single crystals (see the Supplementary data) indicate that two salts show semiconducting behaviors with different resistivity by over two orders of magnitude at room temperature for $(\mathbf{1c})_2\text{Cl}$ ($\rho_{\text{RT}} = 0.14 \text{ \Omega cm}$)¹⁹ and $(\mathbf{1c})_2\text{Br}$ ($\rho_{\text{RT}} = 50 \text{ \Omega cm}$). The activation energy of $(\mathbf{1c})_2\text{Cl}$ ($E_a = 0.04 \text{ eV}$) is also smaller than that of $(\mathbf{1c})_2\text{Br}$ ($E_a = 0.10 \text{ eV}$).¹⁹ These results indicate that the large overlap integral in the q1 direction in $(\mathbf{1c})_2\text{Cl}$ worked as an anisotropic conduction path, whereas the dimeric character of $(\mathbf{1c})_2\text{Br}$ in the a2 direction enhanced hole localization in the dimer, to form the dimer-Mott state with a relatively high resistivity.

In summary, we have successfully synthesized and characterized novel TTF-based functional electron donor systems with a catechol-fused extended π -electronic structure $\mathbf{1a-f}$ and their charge-transfer salts $(\mathbf{1c})_2\text{Cl}$ and $(\mathbf{1c})_2\text{Br}$. The electronic effects induced by the direct fusion of the catechol moiety to the TTF system were evaluated in terms of the redox properties obtained from the CV measurements with the help of the DFT calculations. In both CT salts, two hydroxyl groups in the catechol unit formed intermolecular hydrogen bonds with halide ions, to construct a 1D hydrogen-bonded chain structure. Interestingly the very subtle differences in the hydrogen-bond distances in $(\mathbf{1c})_2\text{Cl}$ and $(\mathbf{1c})_2\text{Br}$ gave rise to the

significant differences in their overall molecular arrangement (β' - and β -structures) and intermolecular interactions as well as the electrical resistivity. These results demonstrated that the structure and physical properties of this system can be readily changed depending on the hydroxyl-group environment of the catechol unit. In order to further investigate structural and electronic features of this system attributable to the robust intramolecular electronic interaction and the flexible hydroxyl-group environment including protonation/deprotonation behaviors, we are now preparing another type of hydrogen-bonded molecular conductors based on $\mathbf{1a-f}$ as well as the o -semiquinone or catecholate-metal complexes. Furthermore the synthesis of a tetraselenafulvalene (TSF) analogue of $\mathbf{1}$ is of interest and is currently underway.

Acknowledgments

This work was partially supported by Grant-in Aid for Scientific Research (B) (No. 20340087) and Grant-in Aid for Scientific Research on Innovative Areas of Molecular Degrees of Freedom (No. 20110007) from the Ministry of Education, Culture, Sports, Science, and Technology, Japan. We also thank Professor H. Yoshizawa (The University of Tokyo) to utilize PPMS (Quantum Design) for the measurement of electrical resistivity and Dr. Y. Okano (the Instrument Center in the Institute for Molecular Science) to use the X-ray diffractometer with Rigaku Mercury CCD.

Supplementary data

Crystallographic data (excluding structure factors) for the structures in this paper have been deposited with the Cambridge Crystallographic Data Centre as supplementary publication CCDC 876709–876711. Copies of the data can be obtained, free of charge, on application to CCDC, 12 Union Road, Cambridge CB2 1EZ, UK, (fax: +44-(0)1223-336033 or e-mail: deposit@ccdc.cam.ac.uk).

Supplementary data (experimental procedures and characterization data for all new compounds, detailed crystallographic data, electrical resistivity, charge estimation, and band structures) asso-

ciated with this article can be found, in the online version, at <http://dx.doi.org/10.1016/j.tetlet.2012.06.020>.

References and notes

- (a) Schukat, G.; Righter, A. M.; Fanghanel, E. *Sulfur Rep.* **1987**, *7*, 155–240; (b) Yamada, J.; Sugimoto, T. *TTF Chemistry: Fundamentals and Applications of Tetrathiafulvalene*; Springer: Heidelberg, 2004.
- (a) Yamada, J.; Akutsu, H.; Nishikawa, H.; Kikuchi, K. *Chem. Rev.* **2004**, *104*, 5057–5083; (b) Iyoda, M.; Hasegawa, M.; Miyake, Y. *Chem. Rev.* **2004**, *104*, 5085–5113; (c) Jeppesen, J. O.; Nielsen, B. N.; Becher, J. *Chem. Rev.* **2004**, *104*, 5115–5131; (d) Gorgues, A.; Hudhomme, P.; Sallé, M. *Chem. Rev.* **2004**, *104*, 5151–5184; (e) Rovira, C. *Chem. Rev.* **2004**, *104*, 5289–5317.
- For typical examples: (a) Blanchard, P.; Boubekeur, K.; Sallé, M.; Duguay, G.; Jubault, M.; Gorgues, A.; Martin, J. D.; Canadell, E.; Auban-Senzier, P.; Jérôme, D.; Batail, P. *Adv. Mater.* **1992**, *4*, 579–581; (b) Dolbecq, A.; Fourmigué, M.; Batail, P. *Chem. Mater.* **1994**, *6*, 1413–1418; (c) Brown, R. J.; Brooks, A. C.; Griffiths, J.-P.; Vital, B.; Day, P.; Wallis, J. D. *Org. Biomol. Chem.* **2007**, *5*, 3172–3182; (d) Batsanov, A. S.; Bryce, M. R.; Cooke, G.; Dhindsa, A. S.; Heaton, J. N.; Howard, J. A. K.; Moore, A. J.; Petty, M. C. *Chem. Mater.* **1994**, *6*, 1419–1425; (e) Moore, A. J.; Bryce, M. R.; Batsanov, A. S.; Heaton, J. N.; Lehmann, C. W.; Howard, J. A. K.; Robertson, N.; Underhill, A. E.; Perepichka, I. F. *J. Mater. Chem.* **1998**, *8*, 1541–1550; (f) Heuzé, K.; Fourmigué, M.; Batail, P. *J. Mater. Chem.* **1999**, *9*, 2373–2379; (g) Devic, T.; Avarvari, N.; Batail, P. *Chem. Eur. J.* **2004**, *10*, 3697–3707; (h) Neilands, O.; Belyakov, S.; Tilika, V.; Edzina, A. *J. Chem. Soc., Chem. Commun.* **1995**, 325–326; (i) Morita, Y.; Maki, S.; Ohomoto, M.; Kitagawa, H.; Okubo, T.; Mitani, T.; Nakasuji, K. *Org. Lett.* **2002**, *4*, 2185–2188; (j) Morita, Y.; Miyazaki, E.; Umemoto, Y.; Fukui, K.; Nakasuji, K. *J. Org. Chem.* **2006**, *71*, 5631–5637; (k) Chen, W.; Cava, M. P.; Takassi, M. A.; Metzger, R. M. *J. Am. Chem. Soc.* **1988**, *110*, 7903–7904; (l) Murata, T.; Morita, Y.; Fukui, K.; Sato, K.; Shiomi, D.; Takui, T.; Maesato, M.; Yamochi, H.; Saito, G.; Nakasuji, K. *Angew. Chem., Int. Ed.* **2004**, *43*, 6343–6346; (m) Murata, T.; Morita, Y.; Yakiyama, Y.; Fukui, K.; Yamochi, H.; Saito, G.; Nakasuji, K. *J. Am. Chem. Soc.* **2007**, *129*, 10837–10846.
- (a) Fourmigué, M.; Batail, P. *Chem. Rev.* **2004**, *104*, 5379–5418; (b) Suzuki, H.; Ichikawa, S.; Yamashita, K.; Kimura, S.; Mori, H.; Nishio, Y.; Kajita, K. *Synth. Met.* **2005**, *154*, 261–264. See also our recent studies on hydrogen-bonded molecular crystals that show the dielectric response; (c) Suzuki, H.; Mori, H.; Yamaura, J.; Matsuda, M.; Tajima, H.; Mochida, T. *Chem. Lett.* **2007**, *36*, 402–403; (d) Ohchi, H.; Takahashi, K.; Yamaura, J.; Takaishi, S.; Mori, H. *Physica B* **2010**, *405*, S341–S343.
- For reviews: (a) Pierpont, C. G.; Buchanan, R. M. *Coord. Chem. Rev.* **1981**, *38*, 45–87; (b) Pierpont, C. G. *Coord. Chem. Rev.* **2001**, *219–221*, 415–433.
- (a) Khan, M. A. *J. Mol. Struct.* **1986**, *145*, 203–218; (b) Winstanley, K. J.; Sayer, A. M.; Smith, D. K. *Org. Biomol. Chem.* **2006**, *4*, 1760–1767; (c) Winstanley, K. J.; Smith, D. K. *J. Org. Chem.* **2007**, *72*, 2803–2815.
- Watson, W. H.; Eduok, E. E.; Kashyap, R. P.; Krawiec, M. *Tetrahedron* **1993**, *49*, 3035–3042.
- Cabezón, B.; Quesada, E.; Esperanza, S.; Torres, T. *Eur. J. Org. Chem.* **2000**, 2767–2775.
- Demeter, D.; Blanchard, P.; Grosu, I.; Roncali, J. *Electrochem. Commun.* **2007**, *9*, 1587–1591.
- Fuji, K.; Ichikawa, K.; Node, M.; Fujita, E. *J. Org. Chem.* **1979**, *44*, 1661–1664.
- The reason why the debenzoylation reaction was performed at this stage is that the debenzoylation after formation of the TTF skeleton was not successful. In addition, reprotection by TBDMS groups was required for the next cross-coupling reaction.
- The X-ray crystal structure of the ethylenedithio derivative **1c** is illustrated in the [Supplementary data](#).
- (a) Fourmigué, M.; Krebs, F. C.; Larsen, J. *Synthesis* **1993**, 509–512; (b) Morand, J. P.; Brzezinski, L.; Manigand, C. *J. Chem. Soc., Chem. Commun.* **1986**, 1050–1052.
- All DFT calculations were performed with Gaussian03 program (revision E.01) Gaussian, Inc., Wallingford CT, 2004; the full reference is listed in the [Supplementary data](#).
- The detailed crystallographic data and molecular structures are shown in the [Supplementary data](#).
- Mori, T. *Bull. Chem. Soc. Jpn.* **1998**, *71*, 2509–2526.
- Mori, T.; Kobayashi, A.; Sasaki, Y.; Kobayashi, H.; Saito, G.; Inokuchi, H. *Bull. Chem. Soc. Jpn.* **1984**, *57*, 627–633.
- The calculated band structures and Fermi surfaces are also illustrated in the [Supplementary data](#).
- The chloride salt (**1c**)₂Cl showed the further smaller resistivity of 0.016 Ω cm under 2.2 GPa at room temperature, however, metallic behavior was not observed probably due to the strong one-dimensionality of the band structure. For detail, see the [Supplementary data](#).